Chemistry & Biology
Article

Visualization of Src Activity at Different Compartments of the Plasma Membrane by FRET Imaging

Jihye Seong,[1] Shaoying Lu,[2] Mingxing Ouyang,[2] He Huang,[2] Jin Zhang,[3] Margaret C. Frame,[4] and Yingxiao Wang[1,2,5,*]
[1]Neuroscience Program
[2]Department of Bioengineering and Beckman Institute for Advanced Science and Technology
Center for Biophysics and Computational Biology, University of Illinois at Urbana-Champaign, Urbana, IL 61801, USA
[3]Departments of Pharmacology and Molecular Sciences, Neuroscience, and Oncology, Johns Hopkins School of Medicine, Baltimore, MD 21205, USA
[4]The Beatson Institute for Cancer Research, Cancer Research UK Beatson Laboratories, Garscube Estate, Switchback Road, Bearsden, Glasgow G61 1BD, UK
[5]Department of Integrative and Molecular Physiology, Center for Biophysics and Computational Biology, University of Illinois at Urbana-Champaign, Urbana, IL 61801, USA
*Correspondence: yingxiao@uiuc.edu
DOI 10.1016/j.chembiol.2008.11.007

SUMMARY

Membrane compartments function as segregated signaling platforms for different cellular functions. It is not clear how Src is regulated at different membrane compartments. To visualize local Src activity in live cells, a FRET-based Src biosensor was targeted in or outside of lipid rafts at the plasma membrane, via acylation or prenylation modifications on targeting tags either directly fused to the biosensor or coupled to the biosensor through an inducible heterodimerization system. In response to growth factors and pervanadate, the induction of Src activity in rafts was slower and weaker, dependent on actin and possibly its mediated transportation of Src from perinuclear regions to the plasma membrane. In contrast, the induction of Src activity in nonrafts was faster and stronger, dependent on microtubules. Hence, Src activity is differentially regulated via cytoskeleton at different membrane compartments.

INTRODUCTION

The nonreceptor tyrosine kinase Src plays critical roles in numerous cellular processes (Martin, 2001). For example, Src kinase regulates cell migration by the phosphorylation of the adaptor protein p130CAS to recruit Crk and DOCK180/ELMO, which can activate Rac1 to induce the formation of lamellipodia at the leading edge of migrating cells (Cote and Vuori, 2007; Hall, 2005; Rodriguez et al., 2003). In addition, Src binds to the autophosphorylated tyrosine 397 of focal adhesion kinase (FAK) via its SH2 domain and phosphorylates tyrosine 925 of FAK. Grb2 can then bind to this site and displace FAK from paxillin, causing focal adhesion turnover in the trailing edge of the cell (Mitra et al., 2005). Src is also involved in the proliferation through the Ras-MAPK pathway and in cell survival through PI3K-Akt signaling (Thomas and Brugge, 1997). To mediate such a variety of cellular signaling transduction, the activation and function of Src kinase require a highly coordinated regulation in space and time. Indeed, Src at its resting state is localized mainly in the endosomes near the perinuclear region and microtubule organizing center (Kaplan et al., 1992). Upon stimulation, active Src can be translocated to the plasma membrane via the actin cytoskeleton (Sandilands et al., 2004). There is also evidence that Src regulates downstream signals differently depending on its subcellular localization. For example, Src induces p190RhoGAP activation and subsequently inhibits RhoA at focal adhesion sites (Thomas and Brugge, 1997), but activates RhoA at podosomes (Berdeaux et al., 2004). Therefore, the visualization of the dynamic activation pattern of Src at subcellular environments will provide critical insight on our understanding of the molecular mechanism regulating cellular functions.

The plasma membrane is not uniform in structure (Simons and Toomre, 2000) and has different nano-size compartments, such as lipid rafts, that are rich in cholesterol, sphingomyelin, and saturated fatty acids (Brown and Rose, 1992). These compartmental structures are involved in the localization and regulation of intracellular signaling molecules (Jacobson et al., 2007; Lasserre et al., 2008). For example, Src family kinases (SFKs) are transported to distinct compartments of plasma membrane through different types of endosomes (Sandilands et al., 2007). SFK members such as Lyn and Fyn can reside in lipid rafts of the plasma membrane (Simons and Toomre, 2000), via their N-terminal sequences after myristoylation and palmitoylation (Zacharias et al., 2002). However, Src kinase has only a myristoylation motif, and it remains controversial whether Src kinase localizes within lipid rafts at the plasma membrane (Arcaro et al., 2007; Hitosugi et al., 2007; Hur et al., 2004; Kasai et al., 2005; Mukherjee et al., 2003; Shima et al., 2003). The detergent extraction method has been widely used to study the lipid rafts because of its detergent-resistant property. In mouse fibroblasts, Src was excluded from the detergent-resistant membrane (DRM) fractions in one study, whereas another publication suggested that Src resides in DRM fraction (Mukherjee et al., 2003; Shima et al., 2003). Different groups also reported different Src localizations in PC12 cells (Hur et al., 2004; Kasai

et al., 2005). This inconsistency is likely attributed to the controversial effects of nonionic detergents used in these reports for isolating DRMs, which, however, might not exactly correspond to lipid rafts in living cells and might include membranes that do not contain rafts before detergent extraction (Lichtenberg et al., 2005; Shaw, 2006). Thus, the development of advanced methods is required to study lipid rafts in live cells.

Previous studies have shown that, based on fluorescence resonance energy transfer (FRET), genetically encoded biosensors are capable of monitoring various cellular events in live cells with high spatial and temporal resolution (Zhang et al., 2002). We previously developed a Src FRET biosensor that can detect Src activity in the cytoplasm (Wang et al., 2005). In this study, this Src FRET biosensor was further coupled to membrane-targeting motifs, either by direct fusion or by an inducible heterodimerization system. As such, the biosensor can be directed to tether at different compartments of plasma membrane, where the local Src activity in live cells can be monitored and quantified in real time. Our results revealed that Src activity is differentially regulated at different compartments of the plasma membrane, mediated by different sets of cytoskeletal components.

RESULTS

A Faster and Stronger Induction of Src Activity at Nonraft Membrane Compartments

We previously developed a FRET biosensor capable of visualizing the spatiotemporal Src activity in live cells (Wang et al., 2005). To monitor the local Src activity in different compartments at the plasma membrane, this Src FRET biosensor was genetically modified to be tethered in or outside of lipid rafts (see Figure S1 available online). It has been shown that lipid modification, including acylation and prenylation, is sufficient to target the proteins into the different microdomains of plasma membrane (Zacharias et al., 2002). The lipid raft-targeting biosensor (Lyn-Src biosensor) was hence constructed by genetically fusing acylation substrate sequences derived from Lyn kinase to the N terminus of the cytosolic Src biosensor (Wang et al., 2005). N-terminal glycine and cysteine in the acylation sequences can undergo myristoylation and palmitoylation (Resh, 1994), which partition the biosensor into lipid rafts (Simons and Toomre, 2000). The nonraft biosensor (KRas-Src biosensor) was developed by introducing prenylation sequences (KKKKKKSKTK**C**VIM) from KRas to the C terminus of the cytosolic Src biosensor. Prenylation on the C-terminal cysteine residue and the neighboring polybasic amino acids can target the biosensor to the nonraft regions (Zacharias et al., 2002). In fact, different mobilization properties of Src biosensors in the microdomains of the plasma membrane were revealed in our recent study, which used fluorescence recovery after photobleaching analysis (Lu et al., 2008). We also conducted an in vitro kinase assay to examine the cytosolic, Lyn-tagged, and KRas-tagged biosensors. The results showed that the responses of these three biosensors are very similar in kinetics and magnitude upon Src phosphorylation (data not shown), suggesting that these modifications of Src biosensor, made by fusing peptides at the N/C terminus, do not affect its function in reporting Src activity. Therefore, FRET changes of the Lyn- and KRas-Src biosensors can be used to monitor Src activity at different compartments of the plasma membrane.

To investigate the spatiotemporal induction of Src activity, we first examined the FRET response of different Src biosensors in response to growth factor stimulations (Figure 1). The results revealed that both epidermal growth factor (EGF, 50 ng/ml) in HeLa cells and platelet-derived growth factor (PDGF, 50 ng/ml) in mouse embryonic fibroblasts (MEFs) induced significant FRET changes of the Src biosensors, with a faster and stronger response from the nonraft KRas-Src biosensor when compared with that of the Lyn-Src biosensor at rafts (Figure 1, Movies S1 and S2). In fact, the nonraft KRas-Src biosensor responded promptly to reach the peak (50%–60% change) within 3–5 min, whereas the response of raft Lyn-Src biosensor was much slower and weaker (10%–20% change). These results suggest a faster and stronger induction of Src activity in nonraft regions at the plasma membrane upon growth factor stimulation.

Recent evidence suggests that growth factors regulate signaling transduction via the activation of receptors and the generation of reactive oxygen species (ROS) such as H_2O_2, which oxidize cysteine residues and subsequently inhibit protein tyrosine phosphatases (Rhee, 2006). ROS have also been shown to enhance Src activity (Boulven et al., 2002; Huyer et al., 1997; Takahashi et al., 2004). This combined effect of phosphatase inhibition and Src kinase activation by ROS can highlight Src phosphorylation efficiency on the biosensors to cause their FRET change. Hence, the differential induction of Src activity at different compartments of the plasma membrane was then examined using the ROS generator pervanadate (PVD, 20 μM), which inhibits tyrosine phosphatases and activates Src kinase (Boulven et al., 2002). Again, the KRas-Src biosensor HeLa cells showed a much faster and stronger FRET change in than the Lyn-Src biosensor (Figure 2A, Movie S3). The CFP/YFP ratio of Lyn-Src biosensor started to increase about 15 min after PVD application, when that of the KRas-Src biosensor had already reached its peak. These significantly distinct time courses in FRET response of the KRas- and Lyn- Src biosensors suggest that raft-associated and non-raft-associated proteins are possibly separated or exchangeable, but stay at the different microdomains with different resident time (Malinska et al., 2003; Zacharias et al., 2002). Similar differences in the responses of the KRas- and Lyn-Src biosensors was also observed in other cell types, including bovine aortic endothelial cell (BAEC) and MEF (Figure S2). These PVD-induced FRET changes of Src biosensors were inhibited in $SYF^{-/-}$ MEF cells (null in Src family kinases: Src, Yes, and Fyn) or after the pretreatment of Src inhibitor PP1 (20 μM) in HeLa cells (Figure S3), confirming that the PVD-induced FRET responses mainly represent the enhanced Src activities. These results suggest that a faster and stronger enhancement of Src activity occurred in nonraft regions at the plasma membrane.

Quantification of the Kinetics and Magnitude of the FRET Responses of Src Biosensors

To further study the different kinetics of the Src phosphorylation efficiency upon PVD in membrane compartments, we quantified the parameters representing the Src activation kinetics based on the velocity curves of FRET change in time. The velocity of FRET change, v_i, was calculated by taking the discrete time derivatives of the normalized CFP/YFP emission ratios. The resulting bell-

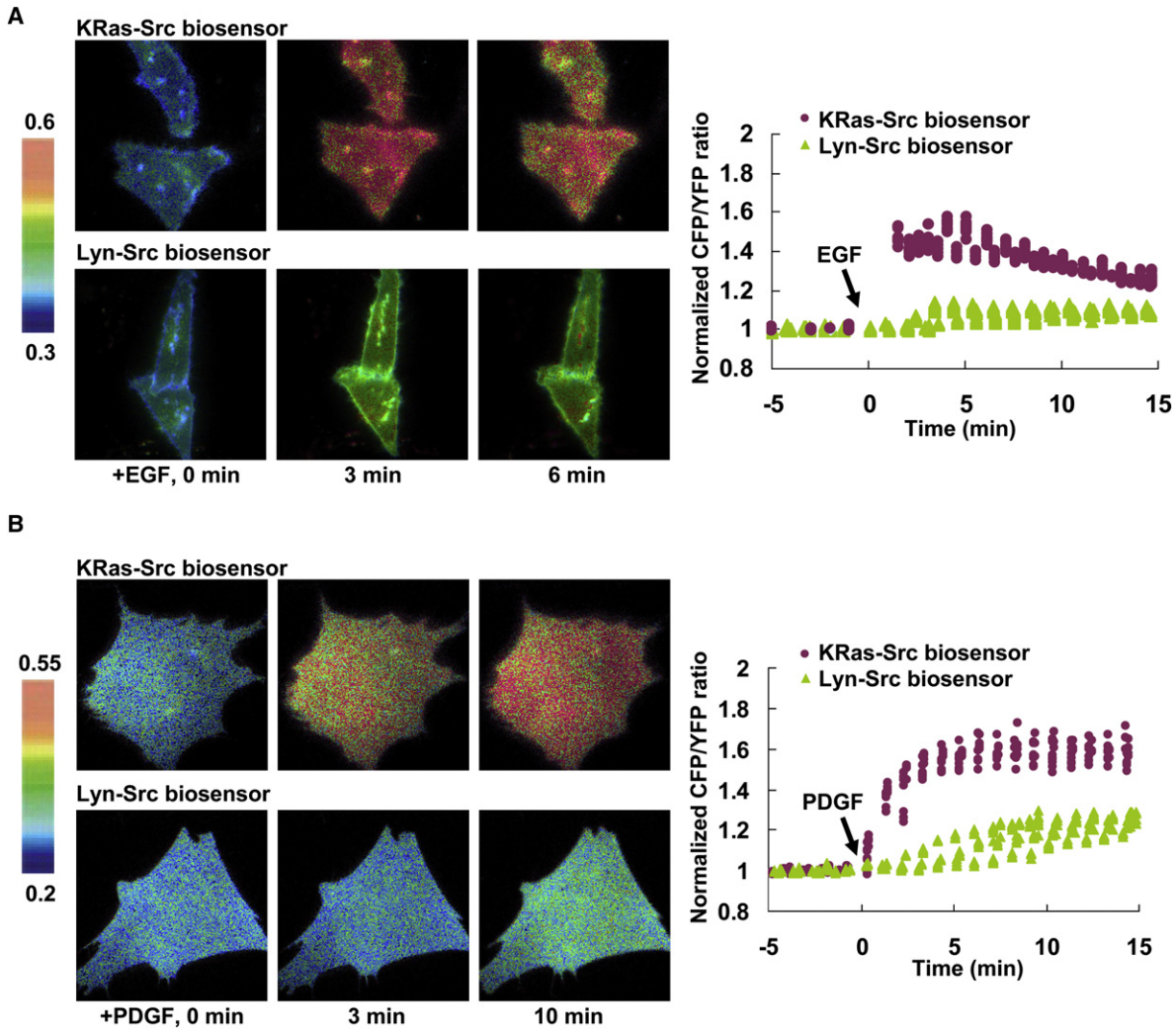

Figure 1. Differential Responses of the Src Biosensor Tethered at Different Compartments of the Plasma Membrane upon Growth Factor Stimulations

The CFP/YFP emission ratio images of KRas- (upper panels) or Lyn-Src biosensors (lower panels) in response to 50 ng/ml EGF in HeLa cells (A) or PDGF in MEF cells (B). The scale bars on the left of the images represent the levels of CFP/YFP emission ratio. Time courses on the right panels represent the normalized CFP/YFP emission ratio of KRas- (purple) and Lyn-Src biosensors (green) before and after stimulations.

shaped velocity curves were fitted by the Gaussian functions given by the following equation:

$$v(t) = A \cdot \frac{1}{\sqrt{2\pi}\sigma} \cdot \exp\left(-\frac{(t-\mu)^2}{2\sigma^2}\right)$$

The parameters A, σ, and μ were estimated by parameter fitting to represent the total FRET change, reaction duration, and the time point where the reaction reaches the maximal velocity, respectively. The onset time of the reaction, T_0, was calculated based on the values of σ and μ ($T_0 = \mu - 1.64485 \times \sigma$, see Supplemental Data). The mean and standard deviation of the parameters were calculated using data from multiple cells and compared between groups.

The KRas-Src biosensor, in comparison to the Lyn-Src biosensor, showed significantly higher value in A (KRas-Src: 0.5734 ± 0.0122; Lyn-Src: 0.3381 ± 0.0088), representing a stronger response, and lower values in σ (KRas-Src: 2.058 ± 0.1169; Lyn-Src: 2.441 ± 0.1459) and T_0 (KRas-Src: 6.936 ± 0.6320; Lyn-Src: 14.042 ± 0.1942), indicating faster and earlier responses (Figure 2C and Table S1). These statistical results confirmed the FRET observations obtained from single-cell imaging. The different dynamics of compartment-targeted Src biosensors was further verified by immunoprecipitation/immunoblotting. As shown in Figure S4, the phosphorylation of the KRas-Src biosensor caused by the enhanced Src activity was detected earlier than that of the Lyn-Src biosensor upon PVD stimulation.

Inducible Heterodimerization System

The membrane-anchoring motif for the Lyn-Src biosensor is at the N terminus, whereas it is at the C terminus for the KRas-Src biosensor (Figure S1). To exclude the possibility that different responses of biosensors were caused by different tagging motifs

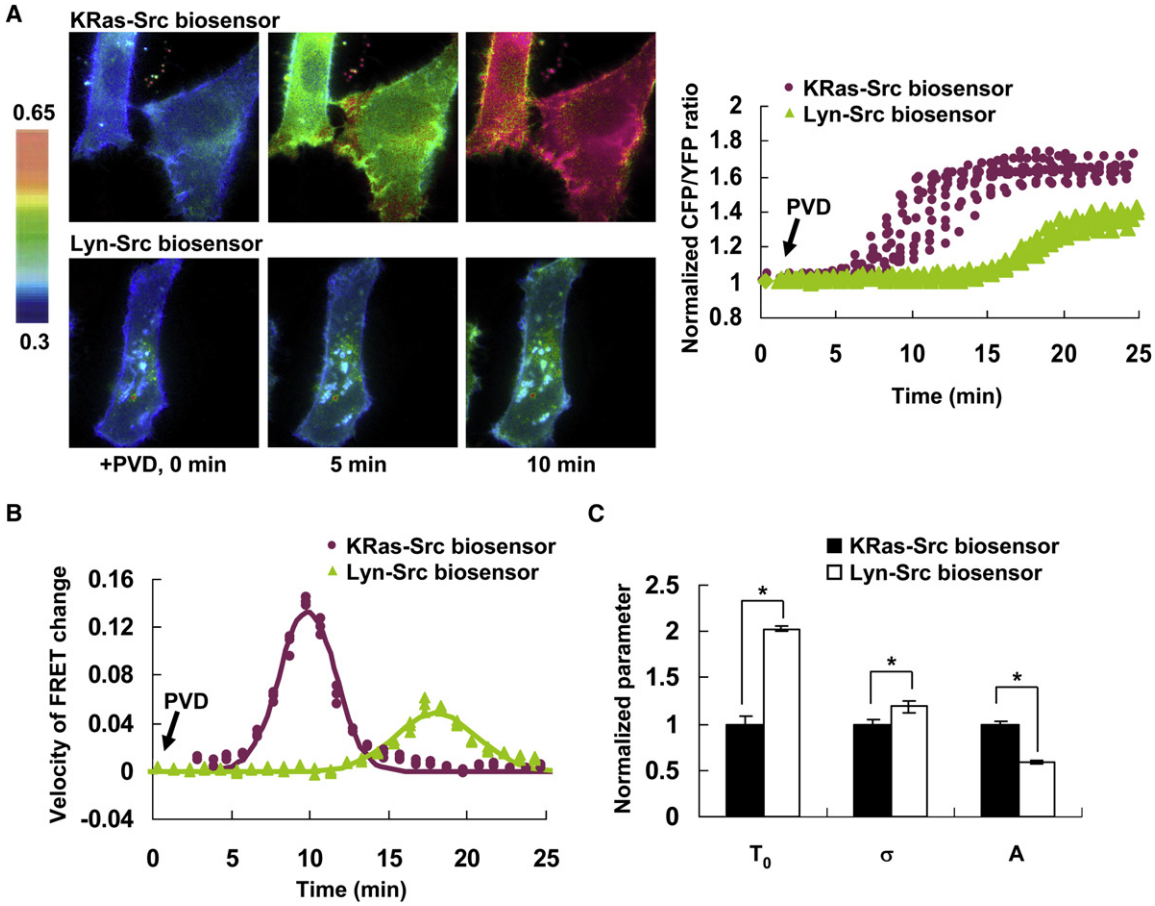

Figure 2. Differential Responses of the KRas- and Lyn-Src Biosensors upon Pervanadate Stimulation

(A) The CFP/YFP emission ratio images of HeLa cells with KRas- or Lyn-Src biosensors in response to pervanadate (PVD) (left panels). Time courses on the right panel represent the normalized CFP/YFP emission ratio of KRas- (purple) and Lyn-Src biosensors (green) before and after stimulations.

(B) The representative velocity curves of FRET signals of KRas- (purple) and Lyn-Src biosensors (green) upon PVD application. Solid lines represent curves of Gaussian function determined by curve-fitting.

(C) The normalized values (mean ± SEM) of T_0, σ, and A for KRas- (black bar) and Lyn-Src biosensors (white bar) determined by parameter fitting (n = 11 and 8, respectively). Asterisks indicate significant differences ($p < 0.05$) between groups.

and/or 3D orientations of the biosensors in relation to the plasma membrane, we applied an inducible heterodimerization system for the membrane localization (Inoue et al., 2005) (Figure 3A). The cytosolic Src biosensor was fused to the FRB domain, and the Lyn- or KRas-targeting motif was fused to FKBP (FRB binding peptides) (Figure S1). When a heterodimerizer AP21967 (1 μM) was introduced into HeLa cells expressing FRB-Src biosensor and the Lyn- or KRas-FKBP peptide, the cytosolic FRB-Src biosensor was successfully recruited to the Lyn- or KRas-FKBP peptides located at the plasma membrane (Figure 3B and Movie S4, data not shown). Again, the subsequent addition of PVD induced a faster and stronger FRET response of the FRB-Src biosensor dimerized with KRas-FKBP than that with Lyn-FKBP (Figure 3C). Statistical results further revealed that the KRas-FKBP/FRB-Src biosensor has higher *A* and lower σ values, in comparison to the Lyn-FKBP/FRB-Src biosensor (Table S1). These results verified that the different kinetics of KRas- and Lyn-Src biosensors originate from their differential compartmental localization, but not from different tagging motifs or 3D orientations.

Two Distinct Populations of Src Kinases Are Regulated by Different Cytoskeletal Components

The plasma membrane is directly connected with and mechanically supported by cytoskeletal structures such as polymerized actin and microtubule filaments (Etienne-Manneville, 2004 ; Rodriguez et al., 2003; Warner et al., 2006). The cytoskeleton has also been known to play important roles in the intracellular movement of molecules, in particular Src translocation (Sandilands et al., 2004, 2007). Thus, we examined the role of the cytoskeletal network in regulating the localization and activation of Src kinase at different membrane compartments.

Because Src kinase can be transported to the plasma membrane via the actin network upon growth factor stimulation (Fincham et al., 1996), we monitored the mobilization of Src kinase (Figure 4A, upper panels; Movie S6) and actin dynamics upon PVD application (Figure 4A, lower panels) using EGFP-conjugated c-Src kinase (Sandilands et al., 2004) and mCherry-conjugated β-actin (Shaner et al., 2004). At the resting state, a large population of Src kinases can be clearly observed near the perinuclear region within endosome-like structures, as

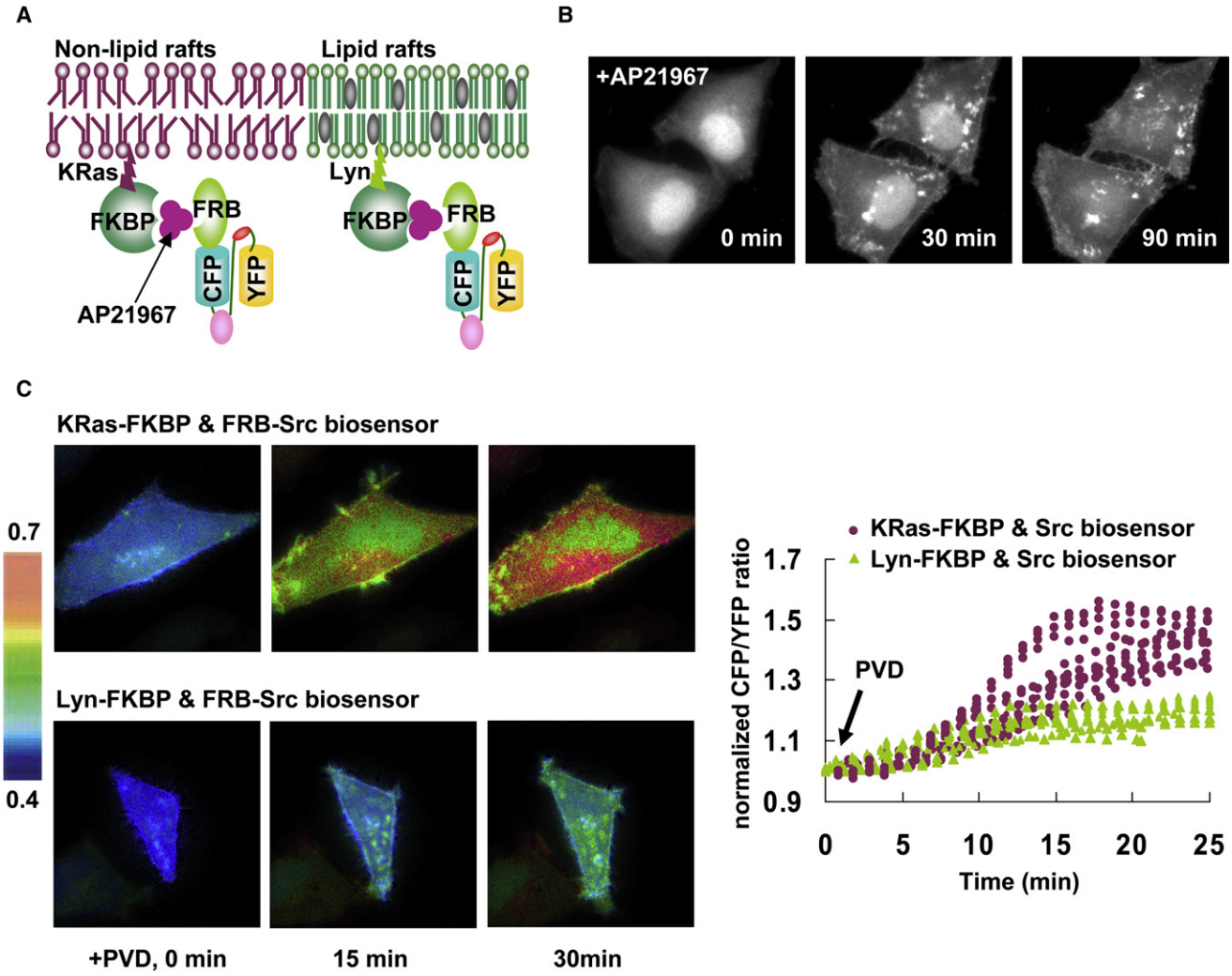

Figure 3. The Responses of Src Biosensors Tethered at the Plasma Membrane through a Heterodimerization System

(A) A cartoon scheme depicting compartmentalization of the biosensors to the plasma membrane by an inducible heterodimerization system.

(B) The CFP images of FRB-Src biosensor before and after AP21697-induced dimerization with Lyn-FKBP.

(C) The CFP/YFP emission ratio images of FRB-Src biosensor dimerized with KRas-FKBP or Lyn-FKBP before and after PVD application for various periods (left panels). Time courses of CFP/YFP emission ratio of FRB-Src biosensors fused to KRas-FKBP (purple) or Lyn-FKBP (green) upon PVD application in HeLa cells (right panel).

previously reported (Sandilands et al., 2004). At 10 min after PVD application, the Src concentration started to decrease in perinuclear regions, with a concomitant increase at cell periphery and plasma membrane ruffles. A colocalization of Src kinase and actin can also be observed at the cell periphery regions after PVD stimulation (Figure 4A). These results suggest that Src kinase is transported to the plasma membrane by actin filaments upon PVD stimulation. Indeed, after pretreatment with cytochalasin D (CytoD) for 1 hr to block actin polymerization, the redistribution of EGFP-wt Src upon PVD was not observed (Figure S5, left panels). The membrane translocation of Src kinase was also blocked by cotransfection of Scar1 WA (a dominant negative mutant of Scar1), which inhibits actin nucleation (Figure S5, middle panels). Interestingly, the inhibition of microtubule by nocodazole (Noco) did not significantly affect the redistribution of c-Src kinase into cell peripheral regions (Figure S5, right panels). These results suggest that Src kinases can translocate to the plasma membrane by utilizing the actin cytoskeleton upon PVD stimulation, similar to previous observations in cells subjected to growth factor stimulation (Fincham et al., 1996).

We then investigated the relationship between different cytoskeletal networks and the responses of Src biosensors (Figures 4B–4E). The PVD-induced FRET response of the Lyn-Src biosensor was significantly inhibited by 1 hr of pretreatment with CytoD (1 μM), but not with 1 μM Noco (Figures 4B and 4D, Figure S6A, and Table S1). CytoD increased the duration of the reaction (σ increased from 2.441 ± 0.1459 to 4.474 ± 0.4830) and decreased total FRET change (A decreased from 0.3381 ± 0.0088 to 0.2049 ± 0.0366) of the Lyn-Src biosensor, suggesting a slower and weaker response (Figure 4B and Table S1). These results suggest that the PVD-induced Src activation at lipid rafts

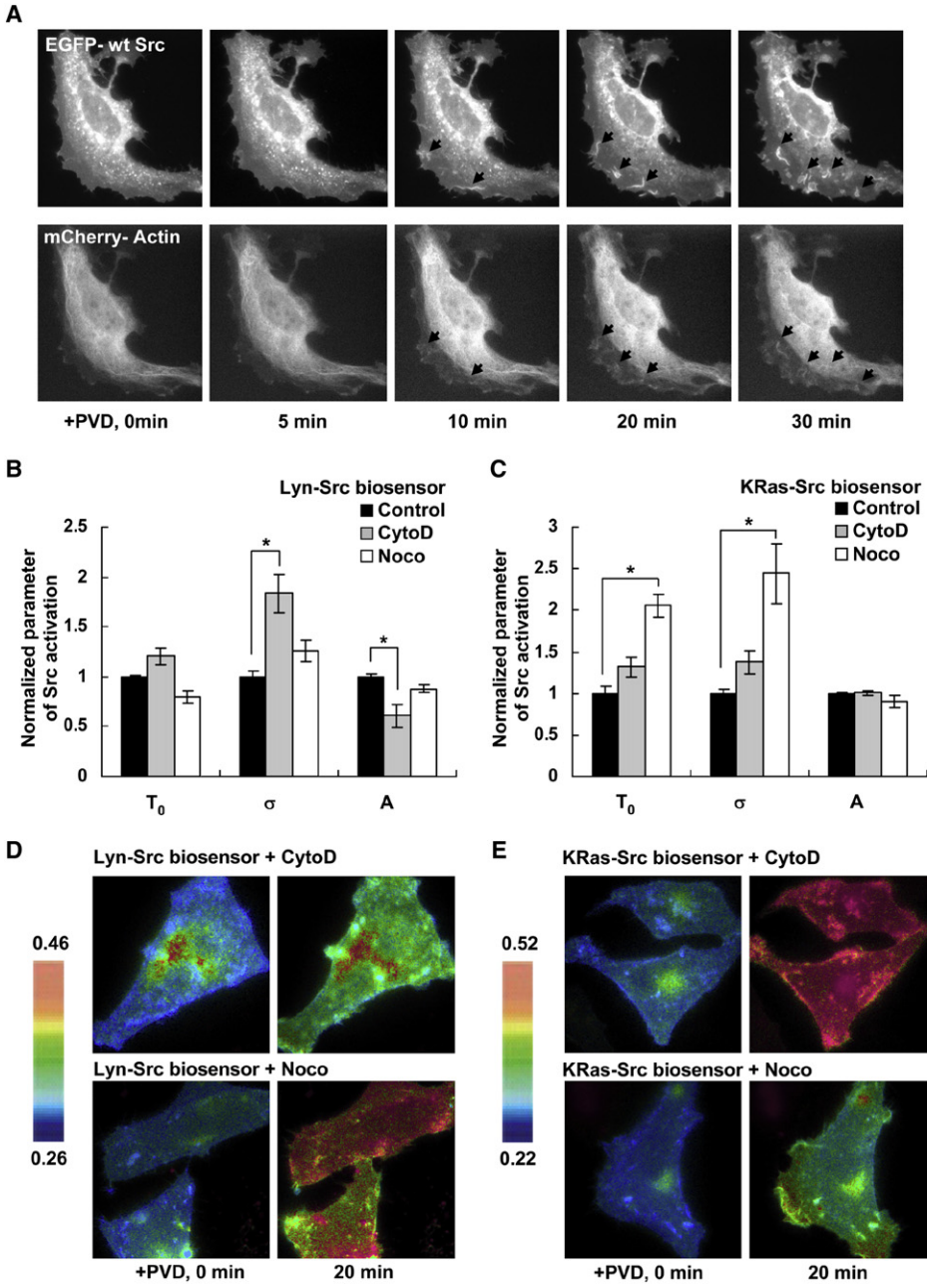

Figure 4. Actin Filaments and Microtubules Differentially Regulate the PVD-Induced Src Biosensor Responses at Different Compartments of the Plasma Membrane

(A) Images of EGFP-conjugated c-Src kinase (upper panels) and mCherry-conjugated β-actin (lower panels) before and after PVD stimulation for various periods. Arrows point to the membrane ruffles where Src kinase and actin fibers are colocalized.

(B and C) Bar graphs represent the normalized values (mean ± SEM) of parameters T_0, σ, and A in different groups of (B) Lyn- and (C) KRas-Src biosensors (n = 8–13). Black, gray, and white bars represent results of biosensors in control cells, and cells treated with cytochalasin D (CytoD) or nocodazole (Noco). Asterisks indicate significant difference with 95% confidence determined by Bonferroni test.

(D and E) The CFP/YFP emission ratio images of HeLa cells expressing Lyn- (D) or KRas-Src (E) biosensors. The cells were exposed to 20 μM PVD after pretreatment with CytoD (upper panels) or Noco (lower panels) as indicated.

is dependent on actin, likely through the Src translocation to the plasma membrane mediated by actin, but not microtubules.

In contrast to the Lyn-Src biosensor, the PVD-induced rapid response of the KRas-Src biosensor was independent of the membrane-translocation of perinuclear Src kinases. The disruption of actin filaments, which blocked the membrane translocation of Src kinase (Figure S5), did not show significant inhibitory effects on the response of the KRas-Src biosensor (Figures 4C and 4E and Table S1). In fact, the KRas-Src biosensor started to respond at around 5 min (Figure 2A), well before a significant

translocation of Src kinases can be observed (Figure 4A). Interestingly, the nonraft Src activity was dependent on microtubules, because the pretreatment with Noco caused a significantly delayed (T_0 increased from 6.936 ± 0.6320 to 14.263 ± 0.9240) and slower (σ increased from 2.058 ± 0.1169 to 5.023 ± 0.7430) response of the KRas-Src biosensor upon PVD treatment (Figure 4C and Table S1). Taxol, a reagent stabilizing microtubules and hence perturbing the dynamics of microtubules, showed similar effects as Noco on the nonraft KRas-Src biosensor (data not shown). The total change of CFP/YFP ratio *A* for the KRas-Src biosensor was not significantly affected by Noco treatment (Figure 4C and Table S1), suggesting that microtubule might affect the onset time and speed, but not the total magnitude of the nonraft Src activation.

We further examined the roles of microtubules and actin cytoskeleton in regulating the responses of the cytosolic Src biosensor. We found that the disruption of actin cytoskeleton or microtubules did not inhibit the FRET response of cytosolic Src biosensor upon PVD stimulation (data not shown). These results suggest that the inhibitory effect of cytoskeletal disruption is specific for the membrane-targeted biosensors and that the phosphorylation of Src biosensor in the cytoplasm does not require an intact cytoskeleton upon PVD stimulation. Thus, the cytoskeleton might be important for the regulation of Src functions at the plasma membrane, but not necessary for the cytosolic processes.

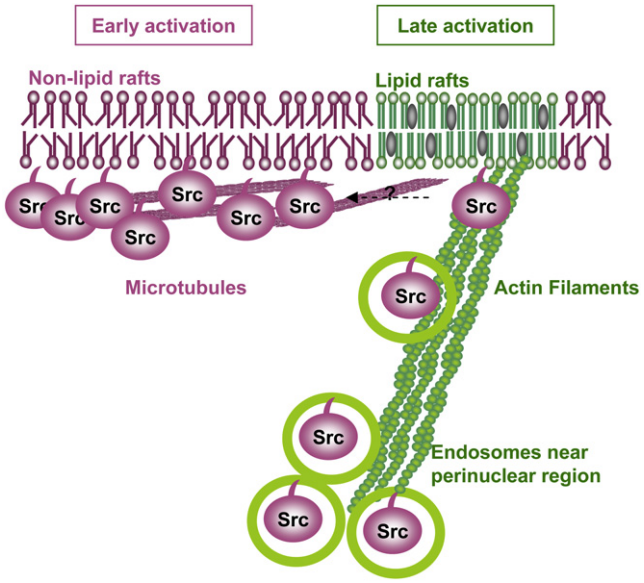

Figure 5. A Proposed Model of Two Distinct Populations of Src Kinases at Plasma Membrane

One population of Src kinases is prestored outside of lipid rafts on plasma membrane at rest state and can be rapidly activated upon stimulation. Another population of Src kinases is located in endosome-like structures around nucleus at rest state, which can translocate to lipid rafts through actin filaments upon stimulation and become activated.

DISCUSSION

Proper subcellular localization of signaling molecules and interaction with correct target molecules are important characteristics of coordinated regulation of the complex signaling network and physiological functions. For example, Src induces the p190GAP activation and inhibits Rho GTPase at the focal adhesion sites (Thomas and Brugge, 1997), whereas it activates Rho GTPase at podosomes (Berdeaux et al., 2004). Lipid rafts have been suggested to serve as the integration site for a variety of signaling pathways. The localization of small GTPase TC10 at lipid rafts is required for the insulin-induced activation and the subsequent regulation of glucose transporter 4 (Watson et al., 2001). Akt in or outside of lipid rafts responded differently to PDGF but not to IGF-1 (Gao and Zhang, 2008). Src kinase also appears to be recruited into lipid rafts by Cbp and inhibited by Csk (Oneyama et al., 2008). Because of the controversial effects of detergent-based extraction of rafts-associated proteins, contradictory results have been reported on the roles of rafts or membrane compartments in determining the Src functions (Arcaro et al., 2007; Hitosugi et al., 2007; Hur et al., 2004; Kasai et al., 2005; Mukherjee et al., 2003; Shima et al., 2003).

In this study, we developed a novel noninvasive method that combines FRET biosensor and statistical analysis to study Src activity in live cells at different compartments of the plasma membrane. Our results indicate that Src activity at the plasma membrane outside of lipid rafts is enhanced in a faster and stronger fashion upon the application of growth factors and PVD. Together with the previous observations that, at resting state, Src kinase is concentrated at the plasma membrane outside of DRM regions (Hitosugi et al., 2007; Kasai et al., 2005; Mukherjee et al., 2003) and at cytoplasm in perinuclear endosomes (Sandilands et al., 2007; Sandilands et al., 2004), our results support the model of two distinct populations of Src (Figure 5). One population of Src kinase exists in nonraft regions on the plasma membrane at the resting state and can be rapidly activated upon stimulation (Hitosugi et al., 2007; Kasai et al., 2005; Mukherjee et al., 2003). The other population of Src is located in perinuclear endosomes at the resting state, and can be transported to lipid rafts upon stimulation in an actin-dependent manner. These differentially regulated Src might direct different cellular functions. Indeed, v-Src at different subcellular locations has recently been reported to regulate differential signaling pathways. For example, v-Src was found at both raft and nonraft regions upon thermoactivation to regulate PI3K/Akt and MAPK/ERK pathways, respectively (de Diesbach et al., 2008). Interestingly, the raft-anchored Akt biosensor has been shown recently to have a faster and stronger response upon PDGF stimulation than that in nonraft regions (Gao and Zhang, 2008). This result suggests that the raft-localization facilitates Akt activation. Together with our observations that Src kinase functions more strongly in nonraft regions at the plasma membrane, it is clear that cells can coordinate the molecular functions and network by controlling the subcellular localization of molecules.

Our results further suggest that these distinct responses of membrane-targeted Src biosensors are mediated by different cytoskeletal networks. The disruption of microtubules had significant effects on the early nonraft Src activation without affecting the translocation and activation of Src at rafts (Figures 4C and 4E; Figure S5), whereas the blockade of actin polymerization by CytoD significantly inhibited the membrane translocation of

Src and its activity at lipid rafts (Figures 4B and 4D; Figure S5). Our results suggest that Src activation at rafts is dependent on the transportation of Src kinases from perinuclear regions to the plasma membrane by actin cytoskeleton, although there is a possibility that actin depolymerization also affects other cellular processes in regulating Src activation. This model is supported by the previous observation that Src can be transported from perinuclear endosome-like regions to cell membrane via actin cytoskeleton and becomes highly activated (Sandilands et al., 2004). In fact, there is ample evidence that lipid rafts are closely connected to actin cytoskeleton. For example, actin-binding proteins such as ezrin and filamin A can serve as bridges between actin cytoskeleton and raft-associated protein such as PAG1 and CD28 (Viola and Gupta, 2007). The raft-associated phosphoinositide lipid $PI(4,5)P_2$ was also shown to regulate actin dynamics by recruiting actin-regulatory molecules such as WASP and ERM (Caroni, 2001). Indeed, actin depolymerization by latrunculin B blocks the proper localization and simulation-induced clustering of raft-anchored fluorescent probes or H-Ras molecules (Chichili and Rodgers, 2007; Murakoshi et al., 2004). The treatment of CytoD to disrupt actin filaments also prevented proper interactions between raft-associated Lyn and IgE-FcεRI (Holowka et al., 2000).

Interestingly, a negative mutant of Scar1 (WA) blocked the responses of both KRas- and Lyn-Src biosensor upon PVD (data not shown). We reasoned that there might be a slow chronic recycling process to maintain the prestored Src population at the plasma membrane outside of lipid rafts (Maxfield and McGraw, 2004), which is dependent on actin-mediated membrane-transportation. The long-term (48 hr) inhibition of actin nucleation by Scar1 WA might block the membrane transportation and prevent an accumulation of Src at the plasma membrane in and outside of lipid rafts, resulting in the inhibition of both the Lyn- and KRas-Src biosensors. It is possible that Src kinases are initially transported to lipid rafts and then translocate into nonraft regions to form the prestored Src population. Short-term (1 hr) treatment with CytoD might only block the acute membrane-translocation of Src toward lipid rafts, and did not affect the prestored Src outside of lipid rafts. Hence, CytoD significantly inhibited the response of Lyn-Src, but not that of the KRas-Src biosensor (Figures 4B–4E).

SIGNIFICANCE

In contrast to the traditional in vitro assays performed in test tubes and cuvettes, the integration of FRET and specific membrane-targeting biosensors allows the quantification of the parameters of enzymatic reactions such as T_0, A, and σ in compartments of plasma membrane, whose sizes are smaller than the resolution of conventional optical fluorescence microscope (the size of single lipid raft is believed to be around 50 nm) (Pralle et al., 2000). The velocity of FRET response in the membrane compartment of each individual cell fits well with the bell-shaped Gaussian function. This result indicates that enzymatic reactions in these different compartments are relatively complex and different from the instant-onset enzymatic reaction described by the Michaelis-Menten model in vitro. These FRET analysis assays can hence advance our systematic and in-depth understanding of enzymatic reactions at subcellular compartments in live cells. The curve fitting and statistical analysis method also provides a general platform to integrate a large quantity of data from single-cell FRET images for the quantification of the molecular kinetics of different signaling cascades. In combination with this statistical analysis approach, our FRET biosensors and live-cell imaging techniques can provide a robust and nonintrusive alternative to biochemical assays.

EXPERIMENTAL PROCEDURES

Cell Culture and Reagents

HeLa and MEF cells were purchased from ATCC. The *Src/Fyn/Yes* triple-knockout MEF ($SYF^{-/-}$) was a generous gift from Dr. Jonathan Cooper (Fred Hutchinson Cancer Research Center). BAECs were isolated from bovine aorta with collagenase. Cell culture reagents were obtained from Invitrogen. Cells were maintained in Dulbecco's modified Eagle's medium supplemented with 10% fetal bovine serum (FBS), 2 mM L-glutamine, 1 U/ml penicillin, 100 μg/ml streptomycin, and 1 mM sodium pyruvate. Cells were cultured in a humidified 95% air, 5% CO_2 incubator at 37°C.

Actin filaments or microtubules were disrupted by incubation for 1 hr with cytochalasin D (Sigma; 1 μM) or nocodazole (Sigma; 1 μM), respectively (Wang et al., 2005). EGF and PDGF were purchased from Sigma.

DNA Constructions and Plasmids

The Lyn-Src biosensor was previously developed and described (Wang et al., 2005). The KRas-Src biosensor was constructed by fusing 14 KRas-prenylation sequences (KKKKKKSKTKCVIM) to the C terminus of Src biosensor using polymerase chain reaction (PCR). For the FRB-Src biosensor, PCR was applied to create HindIII and BamHI sites flanking FRB. The PCR product was fused to the N terminus of Src biosensor in pcDNA3 (Invitrogen). Lyn-FKBP or KRas-FKBP was constructed by PCR of FKBP with the Lyn-acylation sequence (Wang et al., 2005) incorporated into the sense primer or the KRas-prenylation sequence into the antisense primer, respectively. The PCR products of Lyn- or KRas-FKBP were inserted into pcDNA3 using EcoRI/HindIII restriction enzyme sites.

mCherry-β-actin was a kind gift from Dr. Roger Y. Tsien (University of California, San Diego). The expression of mCherry-actin, Scar1WA, and EGFP-wt Src was previously described (Sandilands et al., 2004; Shaner et al., 2004).

Preparation of Pervanadate

Pervanadate solution was prepared as previously described (Huyer et al., 1997). In brief, 10 μl of 100 mM Na_3VO_4 and 50 μl 0.3% H_2O_2 in 20 mM HEPES (pH 7.3) were mixed in 940 μl H_2O. After 5 min, catalase (CalBiochem, 260 U/ml) was added to release excess H_2O_2, which resulted in 1 mM pervanadate.

Inducible Heterodimerization System

The ARGENT™ regulated heterodimerization kit was obtained from ARIAD Pharmaceuticals. The dimerization domain FKBP was conjugated to Lyn-acylation (Wang et al., 2005) or KRas-prenylation sequences for membrane targeting. The other dimerization domain FRB was conjugated to the cytosolic Src biosensor. The cells were cotransfected with the FRB-conjugated Src biosensor and a membrane-targeted FKBP domain (either KRas-FKBP or Lyn-FKBP). Upon the addition of rapamycin analog AP29167 (1 μM), the FRB-conjugated Src biosensor can be induced to associate with the membrane-bound FKBP and be targeted to different compartments at plasma membrane.

Image Acquisition

During imaging, the cells were cultured in cover-glass-bottom dishes and maintained in 0.5% FBS CO_2-independent medium (GIBCO BRL) at 37°C. Images were collected by a Zeiss Axiovert inverted microscope and a cooled charge-coupled device camera (Photometrics, Tucson, AZ) using MetaFluor 6.2 software (Universal Imaging) with a 420DF20 excitation filter, a 450DRLP dichroic mirror, and two emission filters controlled by a filter changer (475DF40 for CFP and 535DF25 for YFP). The mCherry-β-actin images were

collected using a 560DF40 excitation filter, a 595DRLP dichroic mirror, and a 653DF95 emission filter. A neutral-density filter was used to control the intensity of the excitation light. The fluorescence intensity of nontransfected cells were quantified as the background signals and subtracted from the CFP and YFP signals on transfected cells. The pixel-by-pixel ratio images of CFP/YFP were calculated based on the background-subtracted fluorescence intensity images of CFP and YFP by the MetaFluor program to allow the quantification and statistical analysis of FRET responses by Excel (Microsoft) and Matlab (The MathWorks). The emission ratio images were shown in the intensity modified display mode (Wang et al., 2005).

SUPPLEMENTAL DATA

The Supplemental Data include Supplemental Experimental Procedures, Supplemental References, six figures, one table, and five movies and can be found with this article online at http://www.cell.com/chemistry-biology/supplemental/S1074-5521(08)00455-9.

ACKNOWLEDGMENTS

We are very grateful to Roger Y. Tsien for the mCherry cDNA used in this study. This work was supported in part by grants from the Wallace H. Coulter Foundation and Beckman Laser Institute, Inc. (to Y.W.), NIH grants DK073368 and CA122673, and an AHA award (0530217N, to J. Z.).

Received: September 18, 2008
Revised: November 10, 2008
Accepted: November 18, 2008
Published: January 29, 2009

REFERENCES

Arcaro, A., Aubert, M., Espinosa del Hierro, M.E., Khanzada, U.K., Angelidou, S., Tetley, T.D., Bittermann, A.G., Frame, M.C., and Seckl, M.J. (2007). Critical role for lipid raft-associated Src kinases in activation of PI3K-Akt signalling. Cell. Signal. *19*, 1081–1092.

Berdeaux, R.L., Diaz, B., Kim, L., and Martin, G.S. (2004). Active Rho is localized to podosomes induced by oncogenic Src and is required for their assembly and function. J. Cell Biol. *166*, 317–323.

Boulven, I., Robin, P., Desmyter, C., Harbon, S., and Leiber, D. (2002). Differential involvement of Src family kinases in pervanadate-mediated responses in rat myometrial cells. Cell. Signal. *14*, 341–349.

Brown, D.A., and Rose, J.K. (1992). Sorting of GPI-anchored proteins to glycolipid-enriched membrane subdomains during transport to the apical cell surface. Cell *68*, 533–544.

Caroni, P. (2001). New EMBO members' review: actin cytoskeleton regulation through modulation of PI(4,5)P(2) rafts. EMBO J. *20*, 4332–4336.

Chichili, G.R., and Rodgers, W. (2007). Clustering of membrane raft proteins by the actin cytoskeleton. J. Biol. Chem. *282*, 36682–36691.

Cote, J.F., and Vuori, K. (2007). GEF what? Dock180 and related proteins help Rac to polarize cells in new ways. Trends Cell Biol. *17*, 383–393.

de Diesbach, P., Medts, T., Carpentier, S., D'Auria, L., Van Der Smissen, P., Platek, A., Mettlen, M., Caplanusi, A., van den Hove, M.F., Tyteca, D., and Courtoy, P.J. (2008). Differential subcellular membrane recruitment of Src may specify its downstream signalling. Exp. Cell Res. *314*, 1465–1479.

Etienne-Manneville, S. (2004). Actin and microtubules in cell motility: which one is in control? Traffic *5*, 470–477.

Fincham, V.J., Unlu, M., Brunton, V.G., Pitts, J.D., Wyke, J.A., and Frame, M.C. (1996). Translocation of Src kinase to the cell periphery is mediated by the actin cytoskeleton under the control of the Rho family of small G proteins. J. Cell Biol. *135*, 1551–1564.

Gao, X., and Zhang, J. (2008). Spatiotemporal analysis of differential akt regulation in plasma membrane microdomains. Mol. Biol. Cell. *19*, 4366–4373.

Hall, A. (2005). Rho GTPases and the control of cell behaviour. Biochem. Soc. Trans. *33*, 891–895.

Hitosugi, T., Sato, M., Sasaki, K., and Umezawa, Y. (2007). Lipid raft specific knockdown of SRC family kinase activity inhibits cell adhesion and cell cycle progression of breast cancer cells. Cancer Res. *67*, 8139–8148.

Holowka, D., Sheets, E.D., and Baird, B. (2000). Interactions between Fc(epsilon)RI and lipid raft components are regulated by the actin cytoskeleton. J. Cell Sci. *113*, 1009–1019.

Hur, E.M., Park, Y.S., Lee, B.D., Jang, I.H., Kim, H.S., Kim, T.D., Suh, P.G., Ryu, S.H., and Kim, K.T. (2004). Sensitization of epidermal growth factor-induced signaling by bradykinin is mediated by c-Src. Implications for a role of lipid microdomains. J. Biol. Chem. *279*, 5852–5860.

Huyer, G., Liu, S., Kelly, J., Moffat, J., Payette, P., Kennedy, B., Tsaprailis, G., Gresser, M.J., and Ramachandran, C. (1997). Mechanism of inhibition of protein-tyrosine phosphatases by vanadate and pervanadate. J. Biol. Chem. *272*, 843–851.

Inoue, T., Heo, W.D., Grimley, J.S., Wandless, T.J., and Meyer, T. (2005). An inducible translocation strategy to rapidly activate and inhibit small GTPase signaling pathways. Nat. Methods *2*, 415–418.

Jacobson, K., Mouritsen, O.G., and Anderson, R.G. (2007). Lipid rafts: at a crossroad between cell biology and physics. Nat. Cell Biol. *9*, 7–14.

Kaplan, K.B., Swedlow, J.R., Varmus, H.E., and Morgan, D.O. (1992). Association of p60c-src with endosomal membranes in mammalian fibroblasts. J. Cell Biol. *118*, 321–333.

Kasai, A., Shima, T., and Okada, M. (2005). Role of Src family tyrosine kinases in the down-regulation of epidermal growth factor signaling in PC12 cells. Genes Cells *10*, 1175–1187.

Lasserre, R., Guo, X.J., Conchonaud, F., Hamon, Y., Hawchar, O., Bernard, A.M., Soudja, S.M., Lenne, P.F., Rigneault, H., Olive, D., et al. (2008). Raft nanodomains contribute to Akt/PKB plasma membrane recruitment and activation. Nat. Chem. Biol. *4*, 538–547.

Lichtenberg, D., Goni, F.M., and Heerklotz, H. (2005). Detergent-resistant membranes should not be identified with membrane rafts. Trends Biochem. Sci. *30*, 430–436.

Lu, S., Ouyang, M., Seong, J., Zhang, J., Chien, S., and Wang, Y. (2008). The spatiotemporal pattern of Src activation at lipid rafts revealed by diffusion-corrected FRET imaging. PLoS Comput. Biol. *4*, e1000127.

Malinska, K., Malinsky, J., Opekarova, M., and Tanner, W. (2003). Visualization of protein compartmentation within the plasma membrane of living yeast cells. Mol. Biol. Cell *14*, 4427–4436.

Martin, G.S. (2001). The hunting of the Src. Nat. Rev. Mol. Cell Biol. *2*, 467–475.

Maxfield, F.R., and McGraw, T.E. (2004). Endocytic recycling. Nat. Rev. Mol. Cell Biol. *5*, 121–132.

Mitra, S.K., Hanson, D.A., and Schlaepfer, D.D. (2005). Focal adhesion kinase: in command and control of cell motility. Nat. Rev. Mol. Cell Biol. *6*, 56–68.

Mukherjee, A., Arnaud, L., and Cooper, J.A. (2003). Lipid-dependent recruitment of neuronal Src to lipid rafts in the brain. J. Biol. Chem. *278*, 40806–40814.

Murakoshi, H., Iino, R., Kobayashi, T., Fujiwara, T., Ohshima, C., Yoshimura, A., and Kusumi, A. (2004). Single-molecule imaging analysis of Ras activation in living cells. Proc. Natl. Acad. Sci. USA *101*, 7317–7322.

Oneyama, C., Hikita, T., Enya, K., Dobenecker, M.W., Saito, K., Nada, S., Tarakhovsky, A., and Okada, M. (2008). The lipid raft-anchored adaptor protein Cbp controls the oncogenic potential of c-Src. Mol. Cell *30*, 426–436.

Pralle, A., Keller, P., Florin, E.L., Simons, K., and Horber, J.K. (2000). Sphingolipid-cholesterol rafts diffuse as small entities in the plasma membrane of mammalian cells. J. Cell Biol. *148*, 997–1008.

Resh, M.D. (1994). Myristylation and palmitylation of Src family members: the fats of the matter. Cell *76*, 411–413.

Rhee, S.G. (2006). Cell signaling. H2O2, a necessary evil for cell signaling. Science *312*, 1882–1883.

Rodriguez, O.C., Schaefer, A.W., Mandato, C.A., Forscher, P., Bement, W.M., and Waterman-Storer, C.M. (2003). Conserved microtubule-actin interactions in cell movement and morphogenesis. Nat. Cell Biol. *5*, 599–609.

Sandilands, E., Cans, C., Fincham, V.J., Brunton, V.G., Mellor, H., Prendergast, G.C., Norman, J.C., Superti-Furga, G., and Frame, M.C. (2004). RhoB and actin polymerization coordinate Src activation with endosome-mediated delivery to the membrane. Dev. Cell *7*, 855–869.

Sandilands, E., Brunton, V.G., and Frame, M.C. (2007). The membrane targeting and spatial activation of Src, Yes and Fyn is influenced by palmitoylation and distinct RhoB/RhoD endosome requirements. J. Cell Sci. *120*, 2555–2564.

Shaner, N.C., Campbell, R.E., Steinbach, P.A., Giepmans, B.N., Palmer, A.E., and Tsien, R.Y. (2004). Improved monomeric red, orange and yellow fluorescent proteins derived from Discosoma sp. red fluorescent protein. Nat. Biotechnol. *22*, 1567–1572.

Shaw, A.S. (2006). Lipid rafts: now you see them, now you don't. Nat. Immunol. *7*, 1139–1142.

Shima, T., Nada, S., and Okada, M. (2003). Transmembrane phosphoprotein Cbp senses cell adhesion signaling mediated by Src family kinase in lipid rafts. Proc. Natl. Acad. Sci. USA *100*, 14897–14902.

Simons, K., and Toomre, D. (2000). Lipid rafts and signal transduction. Nat. Rev. Mol. Cell Biol. *1*, 31–39.

Takahashi, H., Suzuki, K., and Namiki, H. (2004). Pervanadate-induced reverse translocation and tyrosine phosphorylation of phorbol ester-stimulated protein kinase C betaII are mediated by Src-family tyrosine kinases in porcine neutrophils. Biochem. Biophys. Res. Commun. *314*, 830–837.

Thomas, S.M., and Brugge, J.S. (1997). Cellular functions regulated by Src family kinases. Annu. Rev. Cell Dev. Biol. *13*, 513–609.

Viola, A., and Gupta, N. (2007). Tether and trap: regulation of membrane-raft dynamics by actin-binding proteins. Nat. Rev. Immunol. *7*, 889–896.

Wang, Y., Botvinick, E.L., Zhao, Y., Berns, M.W., Usami, S., Tsien, R.Y., and Chien, S. (2005). Visualizing the mechanical activation of Src. Nature *434*, 1040–1045.

Warner, A.K., Keen, J.H., and Wang, Y.L. (2006). Dynamics of membrane clathrin-coated structures during cytokinesis. Traffic *7*, 205–215.

Watson, R.T., Shigematsu, S., Chiang, S.H., Mora, S., Kanzaki, M., Macara, I.G., Saltiel, A.R., and Pessin, J.E. (2001). Lipid raft microdomain compartmentalization of TC10 is required for insulin signaling and GLUT4 translocation. J. Cell Biol. *154*, 829–840.

Zacharias, D.A., Violin, J.D., Newton, A.C., and Tsien, R.Y. (2002). Partitioning of lipid-modified monomeric GFPs into membrane microdomains of live cells. Science *296*, 913–916.

Zhang, J., Campbell, R.E., Ting, A.Y., and Tsien, R.Y. (2002). Creating new fluorescent probes for cell biology. Nat. Rev. Mol. Cell Biol. *3*, 906–918.